



HAL
open science

Acoustic interaction between 3D fabricated cubic bubbles

Thomas Combriat, Philippine Rouby-Poizat, Alexander A. Doinikov, Olivier Stéphan, Philippe Marmottant

► **To cite this version:**

Thomas Combriat, Philippine Rouby-Poizat, Alexander A. Doinikov, Olivier Stéphan, Philippe Marmottant. Acoustic interaction between 3D fabricated cubic bubbles. *Soft Matter*, 2020, 16, pp.2829–2835. hal-02473441v1

HAL Id: hal-02473441

<https://hal.science/hal-02473441v1>

Submitted on 10 Feb 2020 (v1), last revised 12 Feb 2020 (v2)

HAL is a multi-disciplinary open access archive for the deposit and dissemination of scientific research documents, whether they are published or not. The documents may come from teaching and research institutions in France or abroad, or from public or private research centers.

L'archive ouverte pluridisciplinaire **HAL**, est destinée au dépôt et à la diffusion de documents scientifiques de niveau recherche, publiés ou non, émanant des établissements d'enseignement et de recherche français ou étrangers, des laboratoires publics ou privés.

Cite this: DOI: 00.0000/xxxxxxxxxx

Acoustic interaction between 3D fabricated cubic bubbles[†]

Thomas Combriat,^a Philippine Rouby-Poizat,^a Alexander A. Doinikov,^a Olivier Stephan,^a and Philippe Marmottant^{a*}

Received Date

Accepted Date

DOI: 00.0000/xxxxxxxxxx

Spherical bubbles are notoriously difficult to hold in specific arrangements in water and tend to dissolve over time. Here, using stereolithographic printing, we built an assembly of millimetric cubic frames overcoming these limitations. Indeed, each of these open frames holds an air bubble when immersed into water, resulting in bubbles that are stable for long times and still able to oscillate acoustically. Several bubbles can be placed in any wanted spatial arrangement thanks to the fabrication process. We show that bubbles are coupled acoustically when disposed along lines, planes or 3D arrangement, and that their collective resonance frequency is shifted to much lower values, especially for 3D arrangements where bubbles have higher number of close neighbours. Considering that these cubic bubbles behave acoustically as spherical bubbles of the same volume, we develop a theory allowing to predict the acoustical emission of any arbitrary group of bubbles, in agreement with experiments.

1 Introduction

Acoustic metamaterials present extraordinary properties such as negative index of refraction, or enhanced absorption, giving the hope to create invisibility cloaks around an object or vanishing echoes from it. Typically, such metamaterials contain sub-wavelength resonators that give them unique properties in term of effective density or compressibility^{1,2}. Gas bubbles are good candidates to be these sub-wavelength resonators, because of their remarkable resonance, explained by the much greater compressibility the gas they contain compared to the surrounding liquid. A small amount of bubbles have huge acoustic effect on sound propagation³, that can be experienced in every day life with the hot chocolate effect⁴, where tiny bubbles change dramatically the frequency of sound when tickling the mug. Bubbles can be arranged in static configurations within a solid material, embedded in a aqueous gel⁵ or silicone elastomer^{6,7} with specific positions and sizes. Free gas bubbles in water can be trapped under a net, but with random positions⁸. Bubbles then give super absorption properties to these materials^{9,10}.

Here we would like to introduce meta-materials with gas bub-

bles in water in order to have less viscous friction as possible and still being able to control precisely their sizes and positions. This would provide interesting underwater applications for providing surfaces that could be totally absorbant or acoustically transparent to ultrasonic waves. On a more fundamental level, it is of importance to characterize the resonance of groups of interacting bubbles.

Thanks to the recent evolution of 3D-printing technics we have shown in a previous work¹¹, that it is possible to (i) maintain the position of a gas bubble in water, (ii) stabilise its size, using a single cubic frame where a bubble is trapped.

The present manuscript proposes to incorporate cubic bubbles as building blocks to be arranged into a metamaterial. Our purpose is to find how bubbles couple acoustically to each other, and then to investigate what are the fundamental laws dictating the resonance as a function of the spatial arrangement of bubbles.

2 Methods

We built open cubic frames (external size 3 mm) supported by a loose scaffold (see Fig. 1). This structure was fabricated with a stereolithographic (SLA) 3D-printer (Titan from Kudo3D, “Hard and Tough” type resin, 50 μm resolution). The faces of the cube have square openings 1.94 ± 0.05 mm in height and 1.75 ± 0.05 mm in width (slightly smaller than the 2 mm in design). The actual dimensions of the cubic frames were determined by taking photographs of several structures using a microscope (Leica Z6). The frames were silanized (30 minutes of vapour-phase deposition of trichloro(perfluoro-octyle)silane) in order to make them

^a CNRS / Université Grenoble-Alpes, LIPhy UMR 5588, Grenoble, F-38401, France

* Email: philippe.marmottant@univ-grenoble-alpes.fr

[†] Electronic Supplementary Information (ESI) available: [details of any supplementary information available should be included here]. See DOI: 00.0000/00000000.

[‡] Additional footnotes to the title and authors can be included e.g. ‘Present address:’ or ‘These authors contributed equally to this work’ as above using the symbols: ‡, §, and ¶. Please place the appropriate symbol next to the author’s name and include a

\footnotetext entry in the the correct place in the list.

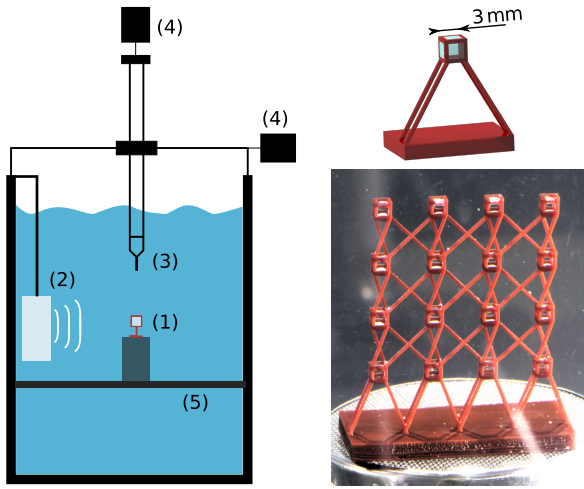


Fig. 1 Left: acoustical setup with: (1) the sample, (2) the loudspeaker, (3) the hydrophone and (4) the moving stage. Top right: 3D view of a typical sample, holding a bubble. Bottom right: photography of a real sample containing a network of 4×4 bubbles.

hydrophobic.

Upon immersion in a water tank, bubbles spontaneously stay inside the cubic frames, because openings are small enough for capillary forces to be stronger than gravity and prevent water from entering. On the opposite, the spaces in the scaffold are large enough to let water invade the structure. In order to minimise the number of parasit bubbles forming outside the cubes, the number of supporting frames was minimised as much as possible in the limit of two supports per cube. In particular, these frames were put in place so that no closed volumes are delimited, giving the “X” shapes that can be seen in Fig. 1 for complex networks.

Each bubble has flat interfaces located on the same plane than the external cube faces. The gas volume V_g of these bubbles is equal to 17mm^3 (using measured dimensions). As previously shown[?] they can, with a good approximation, be considered acoustically equivalent to a spherical bubble of radius $R_{\text{eq}} = 1.6\text{mm}$, with the same volume. Because the interfaces are not curved, the Laplace overpressure inside these bubbles is therefore null and bubbles are much more stable over time. We could study complex arrangements of bubbles as the one shown in Fig. 1 for long times before dissolution, which can occur after a day.

Experiments were performed in a tank ($29 \times 29 \times 50\text{cm}^3$) made of PMMA filled with tap water and a small amount of bleach to prevent the development of micro-organisms. Experiments were performed not before a few days after filling the tank in order for the dissolved gas to reach equilibrium. The sample, denoted (1) in Fig. 1, stood on a mesh cage placed on a steel plate, denoted (5) in Fig. 1, in order for the sample to be situated at the middle of the tank.

The acoustical response of such arrangements was measured by sending acoustic waves with an underwater speaker, broadcasting repeated frequency sweeps. Frequency sweeps ranging from 0.1kHz to 5kHz and lasting 1 second were generated by an arbitrary waveform generator (Handyscope HS5, TiePie) at a sampling frequency of 100kHz . After being amplified (amplifier

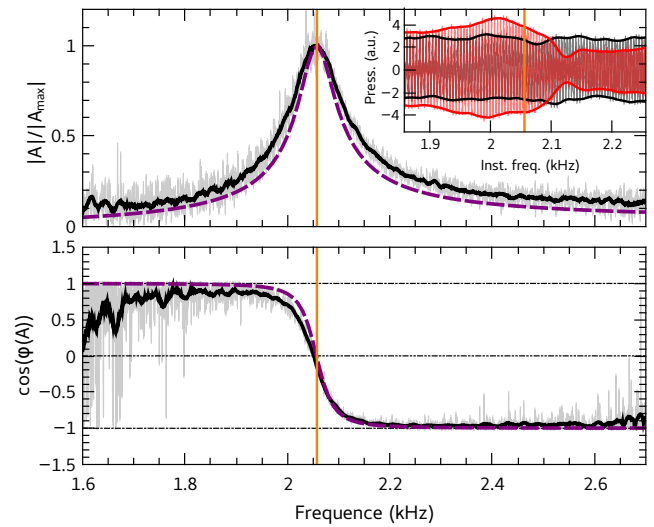


Fig. 2 Amplitude and phase of the acoustic signal A recorded near a single bubble. This signal is the relative difference of the acoustic recording with the recording in the absence of bubbles. Smoothed data (using Savitzky-Golay filter of order 2 on 25 adjacent points) in black are superimposed with the raw data in light grey. The vertical orange line denotes the resonance based on the criteria $\cos(\varphi(A)) = 0$. Numerical simulation for a bubble of radius $R_0 = 1.57\text{mm}$ is also shown it is dashed purple line. Inset in top figure: extract of temporal signals V_{mic}^0 without a bubble (black) and V_{mic} with (red) a bubble present as a function of the instantaneous frequency. Signals envelopes are also shown. The hydrophone is placed approximately 1 cm away from the fixed bubble.

7600M, Krohn Hite Corporation) they were sent to a waterproof loudspeaker (FR 13 WP, Visaton) denoted (2) in Fig. 1. The sound was measured by an hydrophone (8103, Brüel & Kjær) denoted (3) in Fig. 1 and amplified (Nexus Conditioning Amplifier 2692, Brüel & Kjær). This hydrophone can either be attached to a 3D moving stage, denoted (4) in Fig. 1 made from scavenged parts of a 3D printer (Prusa i3 - eMotionTech), allowing to measure acoustic signals at different positions in the tank, or fixed at a given position for the whole experiment.

A signal V_{mic} was recorded by placing a hydrophone in the vicinity of the structure. An additional recording V_{mic}^0 was also performed at the same position, in the absence of the structure. Following Leroy *et al.*[?], we compute the relative bubble contribution using the normalised spectrum

$$A(f) = \frac{\tilde{V}_{\text{mic}} - \tilde{V}_{\text{mic}}^0}{\tilde{V}_{\text{mic}}^0} \quad (1)$$

where \tilde{V}_{mic} and \tilde{V}_{mic}^0 are the Fourier transforms of the signals acquired and f is the frequency.

3 Acoustical response

The emission spectrum of a single bubble is shown in Fig. 2. It features a marked resonant behaviour with a maximum of the amplitude of the normalised emitted pressure $|A|$ and a shift of its phase with respect to the external exciting field from 0 to π , meaning a shift from $\cos(\varphi(A)) = 1$ to $\cos(\varphi(A)) = -1$. Experimentally, we will define the resonant frequency by the condition $\cos(\varphi(A)) = 0$ at resonance. Here it is equal to 2050Hz . This value is very close to the Minnaert’s prediction[?] for a spherical bub-

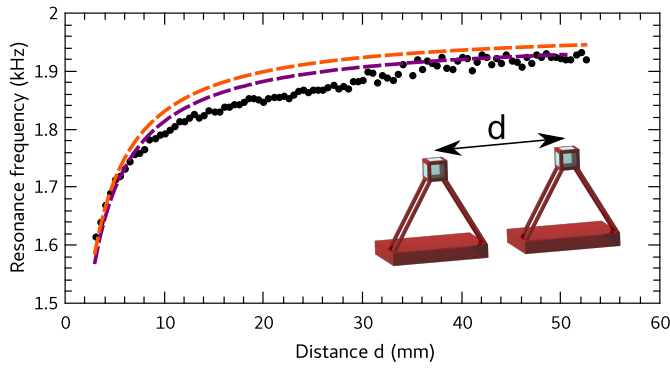


Fig. 3 Evolution of the resonance frequency of a group of two bubbles as a function of their spacing d : dots experimental data, purple line: numerical resolution with $R_0 = 1.65$ mm, orange line: fit using the analytical expression (Eq. 30) $\omega_0^{\text{ana}} = \omega_0 / \sqrt{1 + \frac{R_0}{d}}$ and the Minnaert relation for the frequency, giving $R_0 = 1.65$ mm.

ble of equivalent gas volume: $f_{\text{Minnaert}} = \mathcal{A} / R_{\text{eq}} = 2040$ Hz with $\mathcal{A} = 3.24$ mm/s the Minnaert constant and a radius $R_{\text{eq}} = 1.6$ mm for a spherical bubble having the same gas volume than the cubic bubble. The resonance frequency slowly increases with time (1.7% per hour), which we interpret as a slow dissolution of the bubble. These bubbles have a good quality factor, around $Q = 20$, meaning that the damping ratio $\delta = 1/Q$ is around $5 \cdot 10^{-2}$.

In order to understand the coupling between bubbles, we started with two identical bubbles. One cubic bubble was placed at the sample area of the tank and the other was fixed to a 3D moving stage. Starting from a position of the stage where the bubbles are in contact the distance d between centers was increased by 0.5 mm steps. The hydrophone was placed at the same height than the bubbles, approximately 1 cm away the fixed bubble and outside the way of the moving bubble. Fig. 3 (dots) shows the experimental values of the resonance frequency of such a system with the evolution of the distance d : the resonance frequency decreases when bubbles are approached to each other, as is the case for spherical bubbles⁷.

To go further in the study of the interactions between bubbles, we performed experiments with various numbers of bubbles arranged along a 1D line. We varied the number of bubbles from 2 to 8 bubbles, spaced by $d = 8$ mm. Fig. 4 shows that the experimental resonance frequency diminishes with the number of bubbles.

2D dimensional networks of identical bubbles were also studied. Bubbles were arranged in a matrix configuration, the closest neighbours spaced by 10 mm. Similarly to lines of bubbles, it was found that the resonant frequency decreases with the number of bubbles present in the system (see Fig. 4). The frequency is more reduced with an increasing number of bubbles compared to the linear case because of the larger number of neighbours in 2D arrangements, as this is pinpointed by Fig. 4.

In 3D arrangements the number of neighbours increases dramatically. As every bubble will interact with more bubbles one can expect an even greater reduction of the resonance frequency compared to 1D/2D geometries. In order to specifically pinpoint

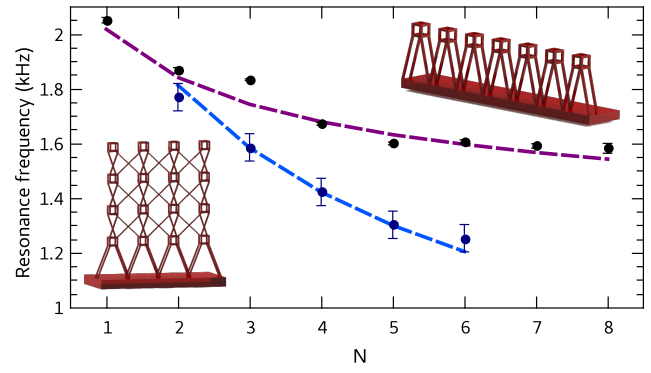


Fig. 4 Evolution of the resonance frequency for lines and matrices of bubbles with the number of bubbles. Black and dark blue points are the experimental frequencies for lines of N bubbles and matrices of $N \times N$ bubbles, respectively. Purple and blue dashed lines are the numerical predictions for these systems, taking $R_0 = 1.6$ mm.

the influence of the dimensions, we have designed arrangements with a central bubble, surrounded by two neighbours in a line (1D line called 1+2), four neighbours in a plane (2D cross 1+4), six neighbours in three directions (3D cross 1+6), see photographs in Fig. 5a-c.

The table in Fig. 5 shows experimental observations up to a 3D arrangement of $3 \times 3 \times 3$ bubbles. This last system has a resonant frequency of around 1 kHz, which represent a huge reduction of the resonant frequency, which is 2 times smaller than the resonant frequency of a single bubble.

4 Modelling

We now attempt to model those observations.

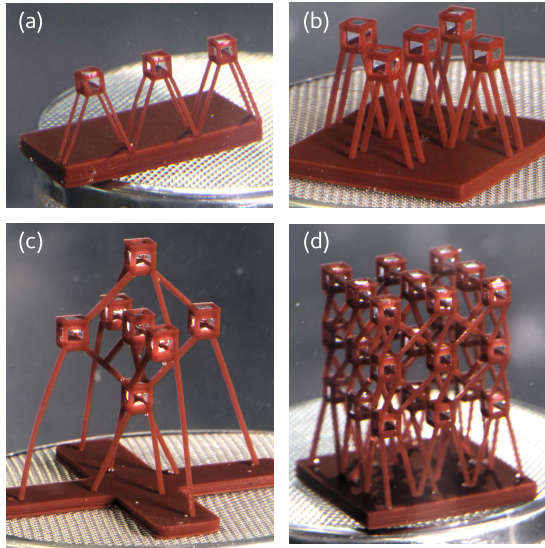
4.1 Bubbles as spherical pulsators

We have previously shown⁷ that the acoustic resonance frequency of a cubic bubble is very close to that of a spherical bubble of same volume. In addition, the emitted field is spatially very close to that of a monopole source, provided the distance d of observation to the cube centre is larger than the cube size. For these reasons we model bubbles as spherical, and the sound emitted by each bubble is described as the one emitted by a spherical bubble whose radius evolves as

$$R_n(t) = R_{n0} + a_n \exp(i\omega t) \quad (2)$$

where R_{n0} is the bubble radius at rest of bubble n and a_n is the amplitude of pulsation ($|a_n| \ll R_{n0}$), in response to a driving acoustic pressure $P_{ac} = P_a \exp(i\omega t)$.

The mechanical equations for the fluid are written in Appendix A. For simplicity we let the interested reader to look at the derivation in this Appendix and we give only the end results here. We find that each bubble, *when alone*, behaves as an oscillator with a resonant pulsation frequency ω_n and damping ratio δ_n (given by Eq. 25 and 26). Note that the resonant frequency is well approximated by the Minnaert equation $f_n = \omega_n / 2\pi = \alpha / R_n$ for millimetric bubbles in water, with $\alpha = 3.24$ m/s. Damping is the consequence of three phenomena: thermal effects, viscosity and



System	f_0^{exp} (Hz)	f_0^{num} (Hz)	f_0^{ana} (Hz)
1+2	1834 ± 50	1748	1703
1+4	1630 ± 60	1581	1593
1+6	1460 ± 100	1454	1468
$3 \times 3 \times 3$	1067 ± 100	1002	

Fig. 5 Top: Pictures of bubble arrangements: 1 + 2 (a), 1 + 4 (b), 1 + 6 (c) and $3 \times 3 \times 3$ (d). The spacing is 8 mm. Bottom: Table presenting the measured resonance frequencies f_0^{exp} of these systems, along with the numerical predictions f_0^{num} and the value of the analytical expressions f_0^{ana} from appendix B using $R_0 = 1.6$ mm.

radiation.

4.2 Interactions between pulsators

Each bubble receives the pressure emitted by neighbour bubbles in addition to the incoming driving field. The model predicts that bubble oscillators when oscillating with an amplitude a_n are coupled by the following set of equations:

$$(\omega^2 - \omega_n^2 - i\omega^2 \delta_n) a_n + \frac{\omega^2}{R_{n0}} \sum_{\substack{m=1 \\ m \neq n}}^N \frac{R_{m0}^2 \exp[-ikd_{nm}] a_m}{d_{nm}} = \frac{P_a}{\rho_0 R_{n0}}, \quad (3)$$

see Appendix A for a full derivation. The coupling term is the second term on the left hand side. In this equation the distance between centres of bubbles n and m is noted d_{nm} . The wavevector is $k = \omega/c$, with c the speed of sound and neglecting here fluid viscosity. The acoustic pressure received by bubbles is assumed to be uniform and equal to P_a , and ρ_0 is the water density. Inverting this system of equations provides the value of the amplitudes a_n . The pressure emitted by all these bubbles is

$$p_{\text{bubbles}}(\mathbf{r}, t) = -\rho_0 c^2 k^2 \exp(i\omega t) \sum_{n=1}^N \frac{R_{n0}^2 a_n \exp[-ikd_{rn}]}{d_{rn}} \quad (4)$$

with $d_{rn} = |\mathbf{r} - \mathbf{r}_n|$, the distance between the microphone of position vector \mathbf{r} and the n^{th} bubble of position vector \mathbf{r}_n .

4.3 Numerical predictions of the acoustic response

Here we assume all bubble to have the same rest radius $R_n = R_0$, and we will adjust this parameter to describe experiments.

The total acoustic pressure amplitude field received by a microphone is $p_{\text{mic}} = P_{\text{ac}} + p_{\text{bubbles}}$, while it is $p_{\text{mic}}^0 = P_{\text{ac}}$ in the absence of bubbles. We can thus model the measured relative spectrum which writes:

$$A^{\text{num}} = \frac{p_{\text{mic}} - p_{\text{mic}}^0}{p_{\text{mic}}^0} = \frac{p_{\text{bubbles}}}{P_{\text{ac}}}. \quad (5)$$

This prediction prediction always showed a peak in amplitude and a change of phase from 0 to π . As in the experiments, we define the numerical resonant frequency f_0^{num} as the first frequency for which which the phase of the response crosses 0, that is the condition $\cos(\varphi(A^{\text{num}})) = 0$ at resonance.

4.4 Comparison with experiments

One bubble The model predicts a spectral response $A^{\text{num}}(f)$ for single bubbles, in agreement with one bubble experiments when choosing the parameter $R_0 = 1.57$ mm (Fig. 2) close to the expected value from the gas volume.

Two bubbles We correctly predict the resonance of a couple of bubbles (Fig. 3) a a function of distance between bubble centers, with a slightly larger $R_0 = 1.65$ mm.

In this special case, it is possible to give a simple analytical prediction (see details in Appendix B, Eq. 30) and it gives a good agreement with experimental and numerical data as it is shown in Fig. 3. For small separation distances d in front of the wavelength (which is around 750 mm at 2 kHz), Eq. 30 is close to the expression $\omega_0^{\text{ana}} \simeq \omega_0 / \sqrt{1 + \frac{R_0}{d}}$, an expression that is classical in litterature[?].

Arrangements in lines or matrices For 1D lines of bubbles and 2D networks (from 2×2 to 6×6) the numerical predictions are in good agreement with experiments, still taking $R_0 = 1.6$ mm, see figure 4.

Arrangements in volumes We also find a good agreement for 3D grids see the table in Fig. 5. Note that because some of these systems have a lot of symmetries, their resonant frequency can be expressed analytically, assuming two groups of bubbles oscillating with the same amplitude: the central one, and the peripheral ones see Appendix B for formulas.

5 Conclusion

As a conclusion, we have shown interaction which takes place between the bubbles downshifts the global resonant frequency of the system and can be predicted using a model of spherical bubbles. This interaction has tremendous effects in 3D arrangements, even when bubbles are parted by distances several times their own sizes (here $d/R_0 = 5$). We found that radius of spherical bubbles used in the simulations varied between 1.57 mm and 1.65 mm depending on the experiments, which we believe is due to imperfections in the fabrication process that changed slightly the inner gas volume, or to a different attachment of the contact line during immersion.

Perspectives will be the global study of larger scale metamateri-

als, with different inter-bubble distances, in order to understand the transmission and absorption properties. In addition further work is needed to detect higher order modes where not all bubbles oscillate in phase.

Author's contributions

T. Combriat designed and 3D printed the frames. He built the tank and a custom made translation stage. He implemented a computer control of devices to send and record acoustic signals. He wrote programs to analyse the signals and performed numerical calculations. P. Rouby-Poizat performed acoustic measurements and analysed their spectrum for the different set of structures. She proposed arrangements with 1+N bubbles. A. Doinikov wrote the theoretical part. O. Stephan initially proposed the idea to built many cubic frames. P. Marmottant derived analytical expression for the case of bubbles having 2,4 and 6 neighbours. He designed and supervised the research. T. C. and P.M. wrote the manuscript.

Acknowledgments

We acknowledge financial support from the European Community's Seventh Framework Programme (FP7/2007-2013) ERC Grant Agreement Bubbleboost no. 614655.

Appendix

A Theory for an assembly of bubbles

We have previously shown[?] that the acoustic resonance frequency of a cubic bubble is very close to that of a spherical bubble of same volume. In addition, the emitted field is spatially very close to that of a monopole source, provided the distance d of observation to the cube centre is larger than the cube size. For these reasons, we will model bubbles as spherical, which should be valid if they are sufficiently distant apart.

We consider a cluster of spherical bubbles located arbitrarily in space. We introduce a global Cartesian coordinate system. The position vector of an arbitrary space point is denoted by \mathbf{r} and has coordinates (x, y, z) . The position vector of the centre of the n^{th} bubble is denoted by \mathbf{r}_n and has coordinates (x_n, y_n, z_n) .

The time-varying radius of the n^{th} bubble is represented as

$$R_n(t) = R_{n0} + a_n \exp(i\omega t) \quad (6)$$

where R_{n0} is the bubble radius at rest and a_n is the amplitude of the bubble pulsation. We assume that $|a_n| \ll R_{n0}$ and solve the problem in the linear approximation.

The liquid around the bubbles is assumed to be viscous and compressible. In the linear approximation, the liquid has a velocity \mathbf{v} and a perturbed density ρ that obey the following equations[?]:

$$\rho_0 \frac{\partial \mathbf{v}}{\partial t} = -\nabla p + \eta \Delta \mathbf{v} + \left(\zeta + \frac{1}{3} \eta \right) \nabla (\nabla \cdot \mathbf{v}) \quad (7)$$

$$\frac{\partial \rho}{\partial t} + \rho_0 \nabla \cdot \mathbf{v} = 0 \quad (8)$$

$$p = c^2 \rho \quad (9)$$

where ρ_0 is the equilibrium liquid density, p is the perturbed liquid pressure, η and ζ are the shear viscosity and the bulk viscosity, respectively, while c is the speed of sound. These equations are the linearized version of the compressible Navier-Stokes equation, the continuity equation and the equation of state of the liquid.

The liquid motion is assumed to be irrotational with $\mathbf{v} = \nabla \phi$, where ϕ is the velocity potential. With a time dependence proportional to $\exp(i\omega t)$ the equations (7)-(9) then provide the Helmholtz equation

$$\Delta \phi + k^2 \phi = 0 \quad (10)$$

where k is given by

$$k = \frac{\omega}{c} \left[1 + \frac{i\omega}{\rho_0 c^2} \left(\zeta + \frac{4}{3} \eta \right) \right]^{-1/2} \quad (11)$$

The velocity potential around the n^{th} bubble is a spherically symmetric solution of equation (10),

$$\phi_n(\mathbf{r}, t) = \frac{A_n}{|\mathbf{r} - \mathbf{r}_n|} \exp(i\omega t - ik|\mathbf{r} - \mathbf{r}_n|). \quad (12)$$

The velocity is then

$$\mathbf{v}_n(\mathbf{r}, t) = -\frac{A_n (1 + ik|\mathbf{r} - \mathbf{r}_n|) (\mathbf{r} - \mathbf{r}_n)}{|\mathbf{r} - \mathbf{r}_n|^3} \times \exp(i\omega t - ik|\mathbf{r} - \mathbf{r}_n|) \quad (13)$$

and the pressure produced by the bubble is

$$p_n(\mathbf{r}, t) = -\frac{i\rho_0 c^2 k^2 A_n}{\omega |\mathbf{r} - \mathbf{r}_n|} \exp(i\omega t - ik|\mathbf{r} - \mathbf{r}_n|) \quad (14)$$

The influence of bubbles on each other's pulsation is taken into account with accuracy up to leading terms with respect to inter-bubble distances and compressibility effects. Within the framework of this accuracy, from the boundary condition for the liquid velocity at the surface of the n^{th} bubble, one obtains

$$A_n = -i\omega R_{n0}^2 a_n \quad (15)$$

To find a_n , we apply the boundary condition for the normal stress at the surface of the n^{th} bubble, which is given by

$$P_{gn} \left(\frac{R_{n0}}{R_n} \right)^{3\kappa_n} = \frac{2\sigma}{R_n} + P_0 + P_{ac} - \sum_{m=1}^N (\sigma_m)_{|\mathbf{r}-\mathbf{r}_n|=R_n} \quad (16)$$

where P_{gn} is the equilibrium pressure of the gas inside the n^{th} bubble, σ is the surface tension, P_0 is the equilibrium pressure in the liquid, $P_{ac} = P_a \exp(i\omega t)$ is the driving acoustic pressure, N is the number of bubbles and $\sigma_m(\mathbf{r}, t)$ is the normal stress produced by the m^{th} bubble in the liquid. Note that in Eq. 16, $\sigma_m(\mathbf{r}, t)$ is taken at the surface of the n^{th} bubble.

In order to take into account deviations from the adiabatic law, the exponent κ_n is defined as[?]

$$\kappa_n = \gamma(\alpha_n + i\beta_n) \quad (17)$$

where γ is the specific heat ratio of the gas. The quantities α_n and

β_n (which are introduced to describe the phase shift between variations of the gas pressure and the bubble volume, caused by heat losses) are the real and imaginary part of κ_n and are calculated by

$$\alpha_n = \left[(1 + \chi_n^2) \left(1 + \frac{3(\gamma - 1)(\sinh X_n - \sin X_n)}{X_n(\cosh X_n - \cos X_n)} \right) \right]^{-1} \quad (18)$$

$$\beta_n = \alpha_n \chi_n \quad (19)$$

where

$$\chi_n = 3(\gamma - 1) \times \frac{X_n(\sinh X_n + \sin X_n) - 2(\cosh X_n - \cos X_n)}{X_n^2(\cosh X_n - \cos X_n) + 3(\gamma - 1)X_n(\sinh X_n - \sin X_n)} \quad (20)$$

$X_n = R_{n0} \sqrt{2\omega/D_{gn}}$, $D_{gn} = K/\rho_n c_{pg}$ is the thermal diffusivity of the gas inside the n^{th} bubble, K is the thermal gas conductivity, c_{pg} is the specific gas heat at constant pressure, $\rho_n = \rho_A P_{gn}/P_A$ is the equilibrium gas density inside the n^{th} bubble and ρ_A is the gas density at the atmospheric pressure P_A .

The complex exponent κ_n in Eq. 16 makes it possible to take account of thermal effects whose contribution to the damping of bubble oscillations is known to dominate the viscous and radiation contributions over a wide range of bubble radii - from a few microns to several hundred microns - unless the driving frequency is considerably above the bubble monopole resonance frequency???

The normal stress produced by the n^{th} bubble is calculated by

$$\sigma_n(\mathbf{r}, t) = -p_n + 2\eta \frac{\partial v_n}{\partial |\mathbf{r} - \mathbf{r}_n|} + \left(\zeta - \frac{2}{3}\eta \right) \nabla \cdot \mathbf{v}_n \quad (21)$$

where $v_n = |\mathbf{v}_n|$. Substitution of Eq. 13, 14 and 15 into Eq. 21 yields

$$\sigma_n(\mathbf{r}, t) = -i\omega R_{n0}^2 a_n \left(\frac{i\rho_0\omega}{|\mathbf{r} - \mathbf{r}_n|} + \frac{4ik\eta}{|\mathbf{r} - \mathbf{r}_n|^2} + \frac{4\eta}{|\mathbf{r} - \mathbf{r}_n|^3} \right) \times \exp(i\omega t - ik|\mathbf{r} - \mathbf{r}_n|) \quad (22)$$

Substituting Eq. 6 and 22 into 16, one obtains

$$P_{gn} = P_0 + \frac{2\sigma}{R_{n0}} \quad (23)$$

$$(\omega^2 - \omega_n^2 - i\omega^2 \delta_n) a_n + \frac{\omega^2}{R_{n0}} \sum_{\substack{m=1 \\ m \neq n}}^N \frac{R_{m0}^2 \exp(-ikd_{nm}) a_m}{d_{nm}} = \frac{P_a}{\rho_0 R_{n0}} \quad (24)$$

which is Eq. 3 in the main text, where we have introduced the resonance frequency of bubbles (when isolated)

$$\omega_n = \frac{1}{R_{n0}} \sqrt{\frac{3\gamma\alpha_n P_{gn}}{\rho_0} - \frac{2\sigma}{\rho_0 P_{n0}}} \quad (25)$$

their damping constant

$$\delta_n = \frac{\omega R_{n0}}{c} + \frac{4\eta}{\rho_0 \omega R_{n0}^2} + \left(\frac{\omega_n}{\omega} \right)^2 \chi_n \quad (26)$$

and the inter-bubble distances $d_{nm} = |\mathbf{r}_n - \mathbf{r}_m|$.

It should be noted that we assume the bubble radii to be much smaller than the acoustic wavelength, $kR_n \ll 1$. Therefore, terms of this order are neglected in Eq. (24), whereas the distances between the bubbles, d_{nm} , can be comparable to and even greater than the acoustic wavelength. Thus, terms of the order kd_{nm} are kept in Eq. (24). We also assume the bubble radii to be small compared to the distances between the bubbles, $R_{n0} \ll d_{nm}$. Therefore, terms of higher order than R_{n0}/d_{nm} are omitted in Eq. (24).

The system of equations Eq. (24) is a system of N algebraic equations in the unknowns a_n . Its solutions gives the values of a_n .

The total pressure produced by all bubbles at the point \mathbf{r} is calculated by

$$p(x, y, z, t) = -\rho_0 c^2 k^2 \exp(i\omega t) \sum_{n=1}^N \frac{R_{n0}^2 a_n \exp[-ikd_{rn}]}{d_{rn}} \quad (27)$$

with $d_{rn} = |\mathbf{r} - \mathbf{r}_n|$, which is Eq. 4 in the main text.

B Analytical predictions for the resonance frequency of 1 + N bubbles

For the specific case of a bubble surrounded by N bubbles at the same distance d , it is possible to find analytical predictions for the resonance frequency, still assuming spherical bubbles. We have tested several configurations.

B.1 Two bubbles: 1+1

Note that for the case a couple of bubbles we can derive an analytical formula for the resonance frequency. - Eq. (3) writes, in a matrix form:

$$\begin{bmatrix} (\omega^2 - \omega_0^2 - i\omega^2 \delta) & \omega^2 \frac{R_0}{d} e^{-ikd} \\ \omega^2 \frac{R_0}{d} e^{-ikd} & (\omega^2 - \omega_0^2 - i\omega^2 \delta) \end{bmatrix} \begin{bmatrix} a_1 \\ a_2 \end{bmatrix} = \begin{bmatrix} \frac{P_a}{\rho R_0} \\ \frac{P_a}{\rho R_0} \end{bmatrix} \quad (28)$$

where we have introduced $\omega_n = \omega_0$ and $\delta_n = \delta$. The solution is:

$$a_1 = a_2 = \frac{P_a / \rho R_0}{\omega^2 \left(1 + \frac{R_0}{d} e^{-ikd} \right) - \omega_0^2 - i\omega^2 \delta} \quad (29)$$

This suggests a natural resonance at

$$\omega_0^{\text{ana}} = \frac{\omega_0}{\sqrt{1 + \frac{R_0}{d} \cos(kd)}} \quad (30)$$

B.2 Three aligned bubbles: 1+2

Now, for simplicity we neglect damping factors δ , and we have assumed the distance d to be extremely small compared to the wavelength $kd \ll 1$ and $e^{-ikd} \simeq 1$.

Owing to the symmetry of the network of three aligned bubbles, we can assume that the amplitudes of the first and last bubbles are equal ($a_1 = a_3$), while the amplitude of vibration of the

central bubble (a_2) might be different. Eq. (24) writes

$$\begin{bmatrix} \left(\omega^2 - \omega_0^2 + \omega^2 \frac{R_0}{d} \right) & \omega^2 \frac{R_0}{d} \\ 2\omega^2 \frac{R_0}{d} & (\omega^2 - \omega_0^2) \end{bmatrix} \begin{bmatrix} a_1 \\ a_2 \end{bmatrix} = \begin{bmatrix} \frac{P_a}{\rho R_0} \\ \frac{P_a}{\rho R_0} \end{bmatrix} \quad (31)$$

The eigen-values of the matrix on the left-hand side are

$$\omega^\pm = \omega_0 \sqrt{\frac{1 + \frac{R_0}{4d} \pm \sqrt{2 + \frac{1}{16} \frac{R_0}{d}}}{1 + \frac{R_0}{2d} - 2 \left(\frac{R_0}{d} \right)^2}} \quad (32)$$

the frequency $\omega_0^{\text{ana}} = \omega^-$ and corresponds to the mode were all bubbles oscillate in phase, while ω^+ is a higher frequency mode that is not excited here.

B.3 A cross of bubbles: 1+4

For the case of four peripheral bubbles all in a plane, still assuming they oscillate in phase, Eq. (24) writes

$$\begin{bmatrix} \left(\omega^2 - \omega_0^2 + \omega^2 \frac{R_0}{2d} (1 + 2\sqrt{2}) \right) & \omega^2 \frac{R_0}{d} \\ 4\omega^2 \frac{R_0}{d} & (\omega^2 - \omega_0^2) \end{bmatrix} \begin{bmatrix} a_1 \\ a_2 \end{bmatrix} = \begin{bmatrix} \frac{P_a}{\rho R_0} \\ \frac{P_a}{\rho R_0} \end{bmatrix} \quad (33)$$

and has a eigen values given by

$$\omega^\pm = \omega_0 \sqrt{\frac{1 + \frac{R_0}{4d} (1 + 2\sqrt{2}) \pm \sqrt{4 + \frac{(1+2\sqrt{2})^2}{16} \frac{R_0}{d}}}{1 + \frac{R_0}{2d} (1 + 2\sqrt{2}) - 4 \left(\frac{R_0}{d} \right)^2}} \quad (34)$$

where $\omega_0^{\text{ana}} = \omega^-$ gives the first resonance frequency.

B.4 A 3D cross of bubbles: 1+6

For the case of six peripheral bubbles, still assuming they oscillate in phase, Eq. (24) writes

$$\begin{bmatrix} \left(\omega^2 - \omega_0^2 + \omega^2 \frac{R_0}{2d} (1 + 4\sqrt{2}) \right) & \omega^2 \frac{R_0}{d} \\ 6\omega^2 \frac{R_0}{d} & (\omega^2 - \omega_0^2) \end{bmatrix} \begin{bmatrix} a_1 \\ a_2 \end{bmatrix} = \begin{bmatrix} \frac{P_a}{\rho R_0} \\ \frac{P_a}{\rho R_0} \end{bmatrix} \quad (35)$$

with eigenvalues for the frequency

$$\omega^\pm = \omega_0 \sqrt{\frac{1 + \frac{R_0}{4d} (1 + 4\sqrt{2}) \pm \sqrt{6 + \frac{(1+4\sqrt{2})^2}{16} \frac{R_0}{d}}}{1 + \frac{R_0}{2d} (1 + 4\sqrt{2}) - 6 \left(\frac{R_0}{d} \right)^2}} \quad (36)$$

where $\omega_0^{\text{ana}} = \omega^-$ gives the first resonance frequency.